Research article

Exploring serum *N*-glycome patterns as candidate non-invasive biomarkers in inguinal hernia

Zhen Cao [a,1], Zejian Zhang [b,***,1], Yuanyang Wang [a,1], Yilin Zhu [c], Zepeng Li [d], Xiaobin Li [a], Yingmo Shen [c], Jie Chen [c,**], Ziwen Liu [a,*]

[a] *Department of General Surgery, Peking Union Medical College Hospital, Chinese Academy of Medical Sciences and Peking Union Medical College, Beijing, China*
[b] *Institute of Clinical Medicine, State Key Laboratory of Complex Severe and Rare Diseases, National Infrastructure for Translational Medicine, Peking Union Medical College Hospital, Chinese Academy of Medical Sciences and Peking Union Medical College, Beijing, China*
[c] *Department of Hernia and Abdominal Wall Surgery, Beijing Chao-Yang Hospital, Capital Medical University, Beijing, China*
[d] *Department of Clinical Laboratory, Peking Union Medical College Hospital, Chinese Academy of Medical Sciences and Peking Union Medical College, Beijing, China*

A R T I C L E   I N F O

A B S T R A C T

Introduction: Although inguinal hernia (IH) is prevalent in elderly males, research on its specific diagnostic biomarkers is limited. Protein *N*-glycosylation is one of the most important and ubiquitous post-translational modifications and often results in a remarkable heterogeneity of protein glycoforms. Protein *N*-glycosylation often changes in a disease and holds great potential for discovering non-invasive biomarkers. This study aimed to gain insights into total serum protein *N*-glycosylation of IH to identify candidate non-invasive biomarkers for diagnosis and subtype classification of IH.
Methods: Linkage-specific sialylation derivatization combined with matrix-assisted laser desorption-tion/ionization time-of-flight mass spectrometry detection was used to analyze serum protein *N*-glycosylation patterns in IH patients and healthy controls.
Results: IH patients had abnormal glycan fucosylation and sialylation compared to healthy controls (HC), of which two glycan traits representing linkage-specific sialylation within mono-antennary glycans showed high potential as diagnostic biomarkers for IH with an area under the curve (AUC) of 0.75. Additionally, serum *N*-glycans were different between indirect IH and direct IH in glycosylation features, namely complexity, fucosylation, galactosylation, sialylation, and α2,6-linked sialylation. Four distinctive glycans between the two subtypes showed good performance with AUC >0.8, suggesting that these glycan traits have potential as biomarkers for subtype classification.

* Corresponding author. Department of General Surgery, Peking Union Medical College Hospital, Chinese Academy of Medical Sciences and Peking Union Medical College, No.1 Shuaifuyuan, Dongcheng District, Beijing 100730, China.
** Corresponding author. Department of Hernia and Abdominal Wall Surgery, Beijing Chao-Yang Hospital, Capital Medical University, No.5 Jingyuan, Shijingshan District, Beijing, 100043, China.
*** Corresponding author. Medical Research Center, State Key Laboratory of Complex Severe and Rare Diseases, Peking Union Medical College Hospital, Chinese Academy of Medical Sciences and Peking Union Medical College, No.1 Shuaifuyuan, Dongcheng District, Beijing, 100730, China.
E-mail addresses: zejianzhang2018@163.com (Z. Zhang), chenjiejoe@sina.com (J. Chen), liuziwen@pumch.cn (Z. Liu).
[1] Z Cao, Z Zhang, and Y Wang have contributed equally to this work and share the first authorship.

Conclusions: We first reported the serum *N*-glycomic features of IH patients. Furthermore, we identified several potential biomarkers for the diagnosis and subtype classification of IH. These findings can deepen the understanding of IH.

1. Introduction

Inguinal hernia (IH) is a malady prevalent in elderly men, and IH repair is among the most routine operations all over the world. More than one in every four men can expect to require IH repair during their lifetime [1]. IHs have been classified as either indirect IH, where the bowel herniates into the scrotum through the defective inguinal ring, or direct IH, where the bowel bulges through weakened abdominal wall muscle [2,3]. The majority of patients usually go to the hospital with symptoms of a palpable mass or pain in the groin. In the clinic, the diagnosis and subtype classification of IH usually relies on physical and ultrasonography examinations. Although current diagnostic techniques are relatively mature, the diagnostic performance relies largely on the clinical experience of the surgeons and radiologists. Additionally, there is no effective screening tool for IH, a small number of patients were diagnosed with strangulated or incarcerated inguinal hernia on initial presentation, which might cause bowel ischemia, necrosis, and perforation. Therefore, there is still no good diagnostic method for screening or detecting IH, and limited information is available regarding their mechanisms [4–6].

N-linked glycosylation is a highly important co- and post-translational modification that involves synergistic actions of a variety of transporters and enzymes [7–9]. *N*-glycosylation is not directly template-driven and indicates remarkable heterogeneity [8,10]. *N*-glycans possess a high degree of diversity and modulate multiple physiological and pathological events [11]. Most human serum proteins are highly glycosylated which makes them a potential reservoir of glycans released from cells and tissues, suggesting that serum protein *N*-linked glycosylation can reflect pathophysiological states [12,13]. Specific protein glycosylation features in serum are associated with various pathological conditions, including liver fibrosis [14], type 2 diabetes [15], Crohn's disease [16], and cancers [17]. The profiling of serum *N*-glycome can enhance the understanding of IH pathogenesis and discover non-invasive biomarkers for early screening and diagnosis. When early screening and diagnosis identify high-risk groups, interventions including appropriate disease management, prophylaxis, and lifestyle modification should be conducted. Nevertheless, little is currently known about serum protein *N*-glycosylation in IH.

Therefore, the detailed structural features and quantitative alterations of serum *N*-glycome between IH patients (including indirect and direct IH) and healthy controls (HC) were investigated. Since the sialic acid function is dependent on the connectivity types, the linkage-specific sialylation derivatization methods differentiating α2,3- and α2,6-linked sialylation on the non-reducing end of *N*-glycans were adopted [18]. Meanwhile, matrix-assisted laser desorption/ionization time-of-flight mass spectrometry (MALDI-TOF MS) was used to detect *N*-glycome structures. This study aimed to unveil serum protein *N*-glycome features that are specific to IH and screen *N*-glycan biomarkers for diagnosis and subtype classification of IH. This study provides a new perspective on potential mechanisms accompanying IH.
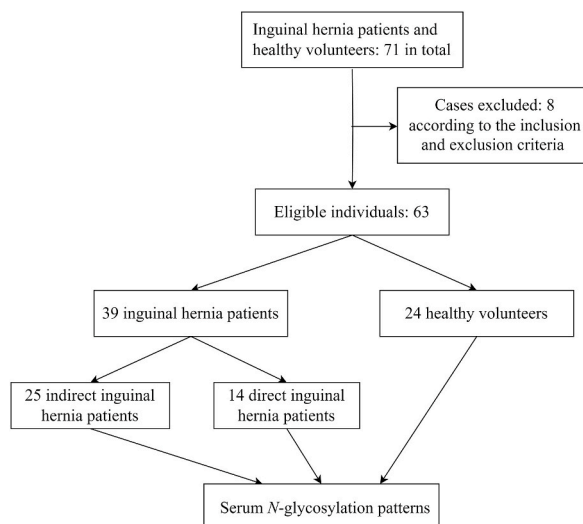

Fig. 1. A flow chart showing the inclusion and exclusion of IH patients and HC volunteers in this work.

2. Methods

2.1. Study population and experimental design

Serum samples obtained from 39 IH patients (25 indirect and 14 direct IHs) and 24 HC volunteers were recruited consecutively from Peking Union Medical College Hospital (Beijing, China) and Beijing Chaoyang Hospital (Beijing, China) between June 2021 to November 2021 and stored at −80 °C. Each individual donated 3–5 mL of blood. The age of the three subgroups was matched where possible. The study design showing the inclusion and exclusion of IH patients and HC volunteers in this work is presented in Fig. 1. The inclusion criteria for the IH group were: (a) age 18–80 years, male sex; and (b) unilateral or bilateral primary indirect or direct IHs. All HC volunteers should have normal biochemical parameters, physical examination, and ultrasonography of the inguinal regions. The exclusion criteria for the IH were: (a) with a history of autoimmune, systemic, blood, or infectious disease; (b) with a previous history of cancer or hernia surgery; (c) with impaired glucose tolerance or diabetes; and (d) with recurrent, incarcerated irreducible hernia, or significant comorbidities. The clinical characteristics of the cohort are shown in Table 1. The study was approved by the Ethics Committee of Peking Union Medical College Hospital and Beijing Chaoyang Hospital (K4094). Informed written consents from all participants were provided.

2.2. Serum N-glycome detection and MS data processing

N-glycans were released from serum specimens after enzymatic treatment based on the protocol described previously [18]. Simply put, the first step was to add 10 μL of 2 % sodium dodecyl sulfate into 5 μL of serum and then incubated at 65 °C for 20 min. Next, the step of glycan release was performed by adding 10 μL of enzyme solution (1 U peptide-N-glycosidase F [New England Biolabs, Inc., USA], 2 % Nonidet P-40, and 2.5 × phosphate-buffered salines) and incubation at 37 °C overnight. Sialic acid residues were derivatized to end products (α-2,3- linked sialic acids were lactonized and α-2,6-linked sialic acids were ethyl-esterified) [18]. Derivatized *N*-glycans were subsequently enriched and purified using hydrophilic interaction liquid chromatography solid-phase extraction (HILIC-SPE) micro-tips according to the previously reported method [17,19]. Thereafter, 1 μL of purified glycans were mixed by matrix (5 mg/mL super-2,5-dihydroxybenzoic acid in 50 % acetonitrile with 1 mM NaOH) on the Anchor chip target plate (MTP AnchorChip TM 384 T F, Bruker Daltonics, Bremen, Germany). After the spots on the target plate dried, glycans were measured by Bruker rapi-fleXtreme MALDI-TOF mass spectrometer (Bruker Daltonics) in positive-ion mode. The instrument was performed using Smartbeam-3D laser and controlled by flexControl 4.0 software (Bruker Daltonics). Bruker Calibration Peptide Standard II is the external calibrant of the instrument. The measurement was recorded at the mass range of 1,000–5,000 *m/z* with a laser frequency of 5,000 Hz. 5,000 times laser shots per shot in a random-walk model were performed.

MS raw data were baseline-subtracted and smoothed using flexAnalysis (Bruker Daltonics). Raw data were converted to. XY format and re-calibrated using MassyTools software (version 0.1.8.1.2) [19]. MS peaks were manually assigned into *N*-glycan structures by Glycoworkbench [20] as well as previously confirmed glycan structures [18]. The list containing 109 glycan structures was finally produced for targeted extraction (output the listed glycan and their corresponding abundance). The peak area (background-corrected) for each glycan and quality control parameters were extracted using the *N*-glycan structures list and MassyTools. After applying quality criteria (S/N > 9, QC score <25 %, ppm error <20, minimum percentage >50 %), 83/109 glycan structures passed the quality criteria and were included for further quantitative analysis (Supplementary Table 1). To combine the exact effect of individual glycan compositions and explain the biological functions, 108 derived *N*-glycan traits which are biochemically possible and detected by the used

Table 1
Clinical and pathological characteristics of all participants.

Characteristics	IH		HC
	Indirect IH	Direct IH	
Sample size	25	14	24
Age [y, $\bar{X} \pm S$]	59.00 ± 14.24	60.14 ± 10.61	58.00 ± 10.06
BMI [kg/m², $\bar{X} \pm S$]	23.13 ± 3.56	23.94 ± 2.47	22.47 ± 3.03
Family history of inguinal hernia [n (%)]			
No	24 (96.0)	14 (100.0)	24 (100.0)
Yes	1 (4.0)	0 (0.0)	0 (0.0)
Smoking history [n (%)]			
No	21 (84.0)	12 (85.7)	19 (79.2)
Yes	4 (16.0)	2 (12.3)	5 (20.8)
ASA score [n (%)]			
I-II	25 (100.0)	14 (100.0)	\
III	0 (0.0)	0 (0.0)	\
EHS classification [n (%)]			
Grade I (<1.5 cm)	5 (20.0)	2 (14.3)	
Grade II (1.5–3.0 cm)	17 (68.0)	7 (50.0)	\
Grade III (>3.0 cm)	3 (12.0)	5 (35.7)	

Abbreviations: IH, inguinal hernia; HC, healthy controls; BMI, body mass index; ASA, American Society of Anesthesiology; EHS, European Hernia Society. Data are presented as mean ± standard deviation or n (%).

technology were calculated from the 83 directly measured glycan based on their common characteristic using RStudio. These derived traits were then used in further studies (Supplementary Table 2).

2.3. Statistical analysis

Since the data were not normally distributed, comparisons were conducted for derived *N*-glycan traits among subgroups (HC vs. IH, HC vs. indirect IH, HC vs. direct IH, and indirect IH vs. direct IH) using nonparametric Mann-Whitney-Wilcoxon test. P values were adjusted by the Benjamini-Hochberg correction. A P value or an adjusted P value threshold of 0.05 was used to indicate a significant difference. The clustered heatmap diagram was constructed using MetaboAnalyst (version 5.0) [21]. GraphPad Prism Software (version 8.4.3) was used to show the data distribution in the scatter dot plot. The diagnostic or predictive (subtype classification) potential of the significantly differed individual glycan traits was further evaluated through the receiver operating characteristic (ROC) curve analyses by calculating the area under the curve (AUC) of ROC. Statistical analyses were performed by SPSS statistics (version 25.0).

3. Results

Serum *N*-glycomic features of IH patients (indirect and direct IH) and matched HC volunteers were profiled by MALDI-TOF-MS. The typical annotated mass spectra of *N*-glycomic profiles from serum samples of indirect IH and indirect IH were presented in Fig. 2,
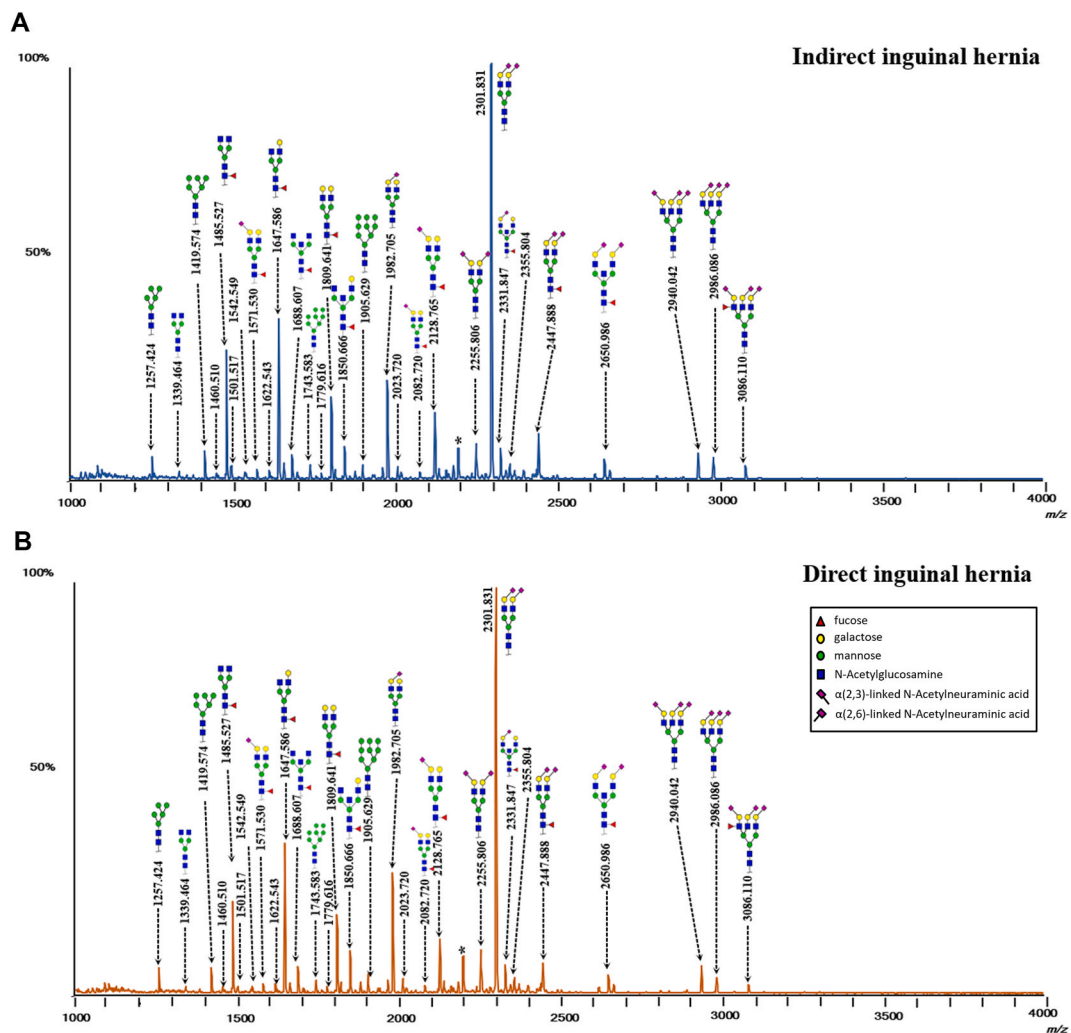

Fig. 2. The typical matrix-assisted laser desorption/ionization time-of-flight mass spectrometry spectra of serum *N*-glycans derived from patients with (A) indirect inguinal hernia, and (B) direct inguinal hernia. Spectra were registered in positive-ion reflectron mode on the Bruker rapifleXtreme mass spectrometer. The major *N*-glycan peaks were labeled and assigned to compositions. The presence of structural isomers cannot be excluded. Asterisk (*) displayed by-products.

indicating differences in peak patterns between the two subtypes. Eighty-three directly detected *N*-glycan structures passed quality criteria, which were grouped into 108 derived *N*-glycan traits based on the common structural characteristics of directly detected *N*-glycans. Features of derived glycan traits included the number of antennae (A), bisection (B), fucosylation (F), galactosylation (G), sialylation (S), α2,3-linked (L), and α2,6-linked sialylation (E) (Supplementary Table 2). The standard deviation (SD) and relative SD (CV) from 10 technical replications of a serum standard sample which were detected together with the cohort samples indicated overall method repeatability. The average CV of the top-20 directly detected glycan traits and all the 108 derived glycan traits were 10.24 % and 8.76 %, respectively (Supplementary Table 3). As derived glycan traits can better interpret the biological significance of glycosylation than directly detected glycans, subsequently we mainly focused on the derived glycan traits [22]. Raw data of directly detected and derived glycan traits for each serum sample were provided in Supplementary Table 4.

3.1. Identification of serum N-glycome alteration in IH compared to HC

To identify the aberrant serum glycan traits in IH, 108 derived *N*-glycan traits were compared among groups (HC vs. IH, HC vs. indirect IH, HC vs. direct IH). A series of *N*-glycan traits were found altered in IH, indirect IH, and direct IH compared to HC (Supplementary Table 5). By taking the intersection of significant differences of serum *N*-glycans between groups (HC vs. IH, HC vs. indirect IH, HC vs. direct IH), 8 serum *N*-glycan traits that were IH-specific were obtained (Fig. 3). Fucosylation within monoantennary glycans (A1LF) and sialylation per galactose within non-fucosylated tetra-antennary sialylation (A4F0GS) were increased in IH than in HC (Table 2). For the linkage-specific sialylation, α2,3-linked sialylation within monoantennary (A1GL and A1FGL), diantennary (A2F0GL), and triantennary (A3GL) species were higher in IH compared to HC (Table 2, Fig. 4A). After multiple testing corrections, we found that the change in A2F0L in direct inguinal hernia compared to the healthy control was not statistically significant. In contrast, α2,6-linked sialylation within (fucosylated) monoantennary species (A1GE and A1FGE) showed significant decreases in IH compared to HC (Table 2, Fig. 4B).

3.2. Performance of serum N-glycan traits for diagnosis of IH

The diagnostic potential of the aberrant *N*-glycan traits in IH mentioned above was further evaluated by the ROC curve (Supplementary Fig. 1). Among all the aberrant *N*-glycan traits, two *N*-glycan traits (A1FGL and A1FGE) showed good performance with the AUCs of 0.791 and 0.791, respectively, in differentiating IH from HC, which showed that two glycan traits have a potential as biomarkers for IH diagnosis (Fig. 4C–D).

3.3. Serum N-glycome patterns among indirect IH and direct IH

Due to certain differences in pathogenesis between indirect IH and direct IH, we also explored the differences in glycosylation between the two groups to improve our understanding of the underlying pathogenesis (Supplementary Table 5). We found that the average number of mannoses on high mannose type glycans (MM) was downregulated in indirect IH compared to that in direct IH
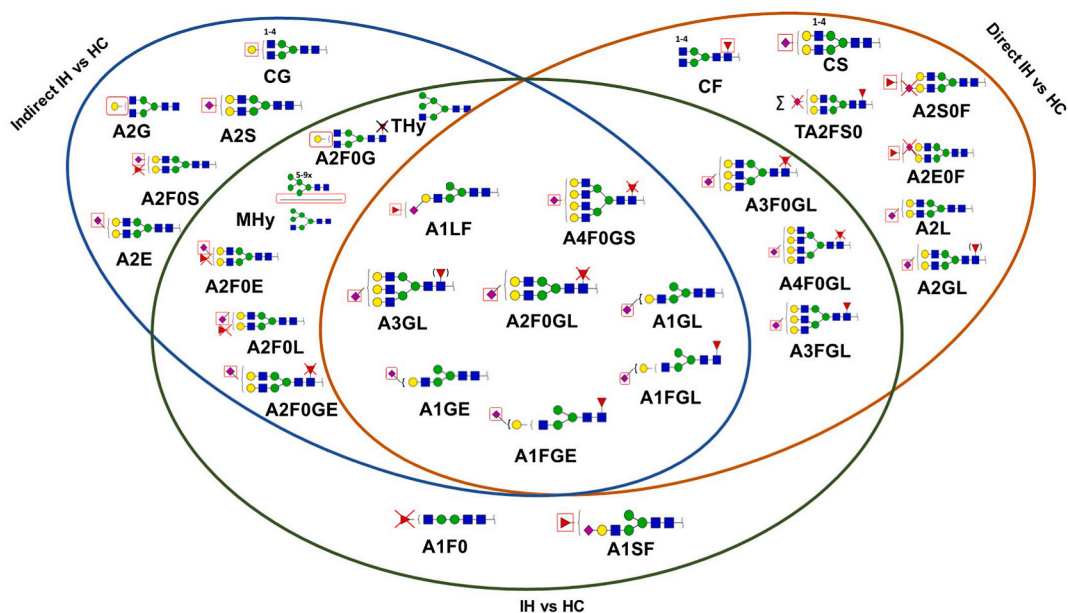

Fig. 3. Venn diagram showing inguinal hernia specific and overlapping serum N-glycans identified as candidate biomarkers. Abbreviations: IH, inguinal hernia, HC health control, Mannose: green circle; galactose: yellow circle; fucose: red triangle; GlcNAc residues: blue square.

Table 2
The differentially expressed derived *N*-glycan traits which were inguinal hernia specific.

Glycan Traits	Descriptions	Median				P value			Adj P value		
		HC	I-IH	D-IH	IH	HC vs. IH	HC vs. I-IH	HC vs. D-IH	HC vs. IH	HC vs. I-IH	HC vs. D-IH
Fucosylation (F)rowhead											
A1LF	in monoantennary (A1) with α2,3- sialylation	0.5045	0.6211	0.6218	0.6211	0.0006	0.0024	0.0054	0.0006	0.0024	0.0056
Sialylation (S)rowhead											
A4F0GS	per galactose in non-fucosylated tetra-antennary glycans (A4)	0.8490	0.8577	0.8563	0.8576	0.0100	0.0238	0.0368	0.0107	0.0263	0.0418
α2,3-linked sialylation (L)rowhead											
A2F0L	in non-fucosylated diantennary (A2)	0.0371	0.0397	0.0410	0.0400	0.0155	0.0340	0.0492	0.0169	0.0404	0.0584
A1GL	per galactose in monoantennary (A1)	0.1305	0.1567	0.1679	0.1632	0.0005	0.0058	0.0011	0.0005	0.0060	0.0011
A3GL	per galactose in triantennary (A3)	0.1887	0.2016	0.2062	0.2026	0.0051	0.0251	0.0093	0.0053	0.0282	0.0097
A2F0GL	per galactose in non-fucosylated diantennary (A2)	0.0385	0.0411	0.0424	0.0419	0.0088	0.0238	0.0293	0.0094	0.0260	0.0327
A1FGL	per galactose in fucosylated monoantennary (A1)	0.2262	0.3067	0.3316	0.3113	0.0001	0.0017	0.0005	0.0017	0.0005	0.0001
α2,6-linked sialylation (E)rowhead											
A1GE	per galactose in monoantennary (A1)	0.8694	0.8432	0.8320	0.8368	0.0005	0.0058	0.0011	0.0005	0.0059	0.0011
A1FGE	per galactose within fucosylated monoantennary (A1)	0.7737	0.6931	0.6682	0.6885	0.0001	0.0017	0.0005	0.0001	0.0017	0.0005

Abbreviations: HC, healthy controls; IH, inguinal hernia; I-IH, indirect inguinal hernia; D-IH, direct inguinal hernia.
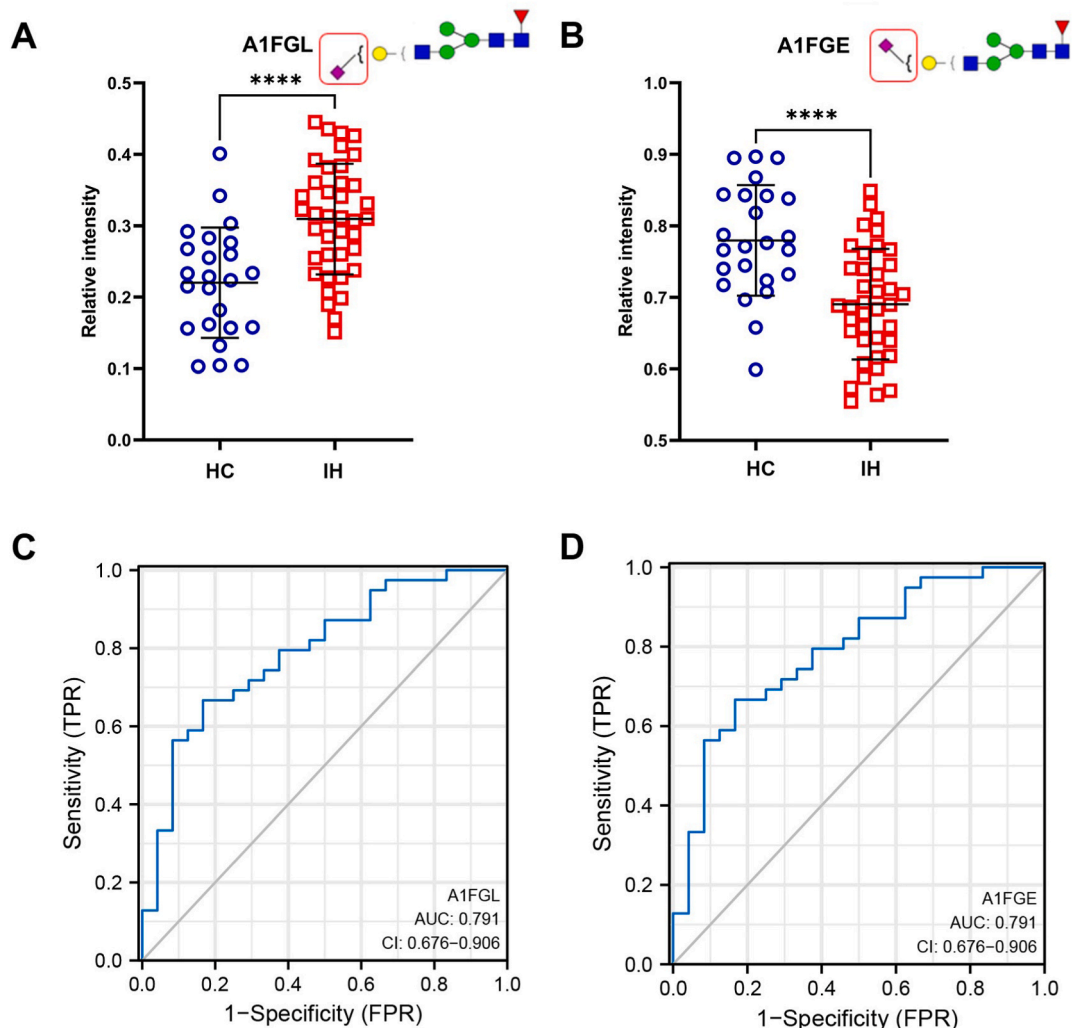
Fig. 4. The expression and ROC curve analysis of two different expressed derived *N*-glycan traits between inguinal hernia patients and healthy control groups. The dot plot expression levels of (A) A1FGL, (B) A1FGE; The ROC curve analysis of (C) A1FGL, (D) A1FGE. The whiskers represent the "median with IQR". **** represents *p*-value <0.0001. Abbreviations: IH, inguinal hernia; HC, health control; AUC, the area under the curve; CI, confidence interval; TPR: true-positive rate; FPR: false-positive rate.

(Table 3). The differences in antennarity (A) of complexity glycans were also found: tetra-antennary complex glycans (CA4) were decreased in indirect IH than in direct IH, with a concomitant increase in diantennary species in indirect IH compared to that in direct IH (CA2; Table 3). Additionally, indirect IH patients showed higher levels of fucosylation than direct IH (CF), which was mainly due to the increase of fucosylation within diantennary species (A2F and A2L0F; Table 3). Consistently, Afucosylated diantennary glycans (A2F0) decreased in indirect IH. In addition to the different fucosylation, indirect IH patients displayed a lower level of galactosylation (CG), which was mainly caused by the decrease of galactosylation within diantennary species (A2G and A2FG; Table 3). As for sialylation linkages, indirect IH patients displayed lower levels of sialylation (CS) than direct IH, primarily because of decreased α2,6-linked sialylation within diantennary species (A2E, A2FE, A2GE, and A2FGE; Table 3). We also found that the changes in A2E0F in indirect inguinal hernia compared to direct inguinal hernia were not statistically significant after applying multiple testing corrections.

3.4. The value of serum N-glycan traits in subtype classification of IH

The value of serum *N*-glycan traits in the subtype classification of IH was further assessed by the ROC curve analyses (Supplementary Fig. 2). Among the differentially expressed *N*-glycan traits between indirect IH and direct IH, four *N*-glycan traits (A2S, A2FS, A2E, and A2FE) displayed accurate performance in distinguishing between the two subtypes with AUCs of 0.803, 0.809, 0.803, and 0.811, respectively, which showed that these glycan traits may be useful for subtype classification of IH.

Table 3
Dysregulated derived *N*-glycan traits in indirect inguinal hernia patients compared to direct inguinal hernia patients.

Glycan Traits	Descriptions	Median		(I-IH vs. D-IH)	
		I-IH	D-IH	P value	Adj P value
General					
MM	Average number of mannoses on high mannose	7.0554	7.0990	0.0242	0.0290
CA2	diantennary species (A2) in complex type glycans	0.8795	0.8663	0.0404	0.0491
CA4	tetra-antennary species (A4) in complex type glycans	0.0149	0.0166	0.0071	0.0076
Fucosylation (F)					
CF	in complex type	0.4204	0.3739	0.0065	0.0069
A2F0	Afucosylated diantennary(A2)	0.5712	0.6169	0.0128	0.0149
A2F	in diantennary (A2)	0.4288	0.3831	0.0128	0.0147
A2L0F	in diantennary species (A2) without α2,3-sialysation	0.4293	0.3832	0.0109	0.0121
Galactosylaiton (G)					
CG	in all complex	0.9262	0.9428	0.0109	0.0123
A2G	in diantennary (A2)	0.8457	0.8741	0.0077	0.0084
A2FG	in fucosylated diantennary (A2)	0.6762	0.7105	0.0177	0.0210
Sialylation (S)					
CS	in all complex	0.7548	0.7986	0.0049	0.0052
A2S	in diantennary (A2)	0.6223	0.6730	0.0019	0.0019
A2FS	In fucosylated diantennary (A2)	0.2994	0.3433	0.0016	0.0016
A2GS	per galactose in diantennary (A2)	0.7330	0.7641	0.0128	0.0151
A2FGS	per galactose in fucosylated diantennary (A2)	0.4466	0.4828	0.0054	0.0057
α2,6-linked sialylation (E)					
A2E	in diantennary (A2)	0.5801	0.6247	0.0019	0.0020
A2FE	in fucosylated diantennary (A2)	0.2525	0.2860	0.0014	0.0014
A2GE	per galactose in diantennary (A2)	0.6855	0.7124	0.0109	0.0122
A2FGE	per galactose in fucosylated diantennary (A2)	0.3749	0.4019	0.0100	0.0110
IgG-specific					
TA2FS0	Fucosylated, non-sialylated diantennary species within total glycans. Mostly derived from IgG	20.5273	16.1902	0.0031	0.0032

Abbreviations: I-IH, indirect inguinal hernia; D-IH, direct inguinal hernia.

4. Discussion

IH is one of the common conditions that usually occur in the groin area in elderly men. The primary risk factors for IH include male gender, age, family history, previous contra-lateral hernia, abnormal collagen metabolism, and low body mass index [23–26]. At present, the IH diagnosis is confirmed by physical and ultrasonography examination. Surgery remains the only curative treatment. Although IHs possess good diagnostic and therapeutic systems, limited information is available on mechanisms and specific diagnostic or subtype classification biomarkers. Continued research and better understanding will improve the stratification and timing of preventive and therapeutic measures by using biological information and biomarkers. Apart from genomics, deciphering changes in protein glycosylation has been of paramount importance not only to know the underlying mechanisms of IH progression but also to discover useful biomarkers. Currently, serum protein *N*-glycans have been determined as biologically significant, and have emerged as the showcase of novel biomarkers for diverse diseases [13,17,27,28]. Hence, the present study explored the application of MALDI-TOF MS technology for quantitative assessment of serum protein *N*-glycans from IH patients and matched controls including linkage-specific sialylation alterations to reveal the characteristics of glycosylation in IH and screen novel biomarkers for the diagnosis and subtype classification of IH.

The comprehensive analysis of serum protein *N*-glycosylation in IH (indirect IH and direct IH) and HC was represented for the first time. To reveal the disease-specific *N*-glycome phenotype of IH, explore underlying mechanisms of IH, and discover potential bio-markers, 108 derived *N*-glycan traits were compared between groups (HC vs. IH, HC vs. indirect IH, HC vs. direct IH). After careful data processing and analysis steps, 8 derived *N*-glycan traits were found to specifically distinguish IH patients from HC, involving fuco-sylated and sialylated glycan traits. Fucosylation is an important modification of the *N*-glycans and is regulated by various fucosyl-transferases. The secreted protein acidic and rich in cysteine (SPARC) can modulate interactions between extracellular matrix (ECM) and cells in many physiological processes. A previous study demonstrated that the core fucosylation of *N*-glycan in SPARC could regulate protein-binding affinity with extracellular matrix collagen [29]. This indicated that alterations in protein fucosylation might play an important role in regulating ECM collagen in IH patients. Regarding sialylation, we found sialylation per galactose within non-fucosylated tetra-antennary glycans was higher in IH compared to HC. Our MS-based approach included the discrimination of different types of terminal sialic acid (α2,3-linked and α2,6-linked) and enabled the identification of the aberrant linkage-specific sialylation in IH. Terminal sialic acids involve many cellular functions, and changes in their biosynthesis or degradation can be involved in degenerative disorders, such as inflammatory disorders, diabetes, or osteoarthritis disease, by regulating immunological and inflammatory functions, affecting ligands, and masking antigenic sites [30–32]. The inflammatory conditions caused by non-infectious etiologies were confirmed by the high values of inflammatory markers (ferritin, D-dimer, procalcitonin, C-reactive protein), normal neutrophil-to-leukocyte ratio, and specific symptoms. The specific symptoms included pain, mobility limitation, and so on. Additionally, high-sensitivity C-reactive protein is a well-established nonspecific marker of systemic inflammation that has been correlated with pain and joint disease. Therefore, inflammatory conditions could be readily identified by surgeons based on the specific

symptoms, signs, and findings on ancillary investigations. Previous studies indicate that the onset of osteoarthritic cartilage degradation is caused by factors that shift the expression of α2,6-linked to α2,3-linked sialylated glycoproteins in chondrocytes. The cartilage is formed by the ECM of collagen II. Cevik et al. also reported that joint hypermobility syndrome which had collagen tissue damage and turnover characteristics was related to IH in children [33]. Intriguingly, IH was strongly related to the type of sialic acid linkage in our study. The expression of α2,3-linked sialylation types was higher and α2,6-linked sialylation was lower in IH samples relative to HC samples and indicate the same trend as osteoarthritis. Therefore, we speculate that the onset of IH may be promoted by factors that shift the expression of α2,6-linked to α2,3-linked sialylated glycoproteins and affect local collagen, thus warrants further investigation. Combining the above information, we found that serum IH-specific N-glycan traits were associated with ECM alteration, which might be an important factor in the process of IH formation. Furthermore, ROC analyses independently confirmed that two altered linkage-specific sialylation glycans (A1FGL and A1FGE) had potential as diagnostic biomarkers for IH. We found that A1FGL and A1FGE indeed resulted in completely the same AUC values. This might be due to the model or sample number limitation. However, this needs further validation studies in large cohorts.

Due to certain differences in the pathogenesis of indirect IH and direct IH, we compared the N-glycomes of the two subtypes to discover glycan biomarkers for subtype classification and explore the underlying mechanisms. Structurally, the majority of the discriminative glycans between the two types are attributed to complexity, fucosylation, galactosylation, sialylation, and α2,6-linked sialylation glycan types. Our investigation of the distinction of N-glycan profiles in indirect and direct IH might point at pathophysiological processes involving many proteins, as we discuss below. As we have mentioned earlier, protein fucosylation changes may play important roles in regulating ECM collagen. What's more, the fucosylation level is substantially higher in indirect IH patients compared to direct IH, suggesting that indirect IH patients may have significant changes in the ECM. Galactosylation occurs through a series of beta-1,4-galactosyltransferases. Galactosylation in serum has been associated with age and inflammatory diseases [34,35]. Furthermore, decreased IgG-derived galactosylation has been linked with immune disorders, inflammation, and aging [35,36]. The decreased galactosylation within diantennary glycans (A2G, A2FG) in indirect IH compared to direct IH may be due to the aberrant IgG-derived glycans, which indicated that indirect IH has a more pronounced proinflammatory phenotype than direct IH. Amato et al. have biopsied and examined tissue specimens from the edge of the internal inguinal ring in eight patients with indirect IH. The results showed that the internal inguinal ring had remarkable degenerative changes, including vascular congestion, fibrohyaline degeneration of muscle fibers, phlogistic infiltration, and so on [37]. Sialylation is directly involved in the activation of the immune system. Abnormal sialylation has been previously found in inflammatory, autoimmune diseases, and cancer [38]. Though most glycan traits containing sialylation were altered in IH, our findings suggest that these alterations in sialylation were partially driven by α2,6-sialyltransferases. ST6Gal1 is the key enzyme responsible for the biosynthesis of α2,6-linked sialylation in N-glycans. The insufficiency of circulatory ST6Gal1 is associated with overly robust inflammatory and exaggerated inflammatory cell production [39,40]. Therefore, we hypothesize that obvious abnormal sialylation including α2,6-linked sialic acids in indirect IH patients was associated with inflammatory changes. The phlogistic elements could represent a reason for the contractile incompetence of the internal inguinal ring which leads to the IH. Notably, four distinctive glycans (A2S, A2FS, A2E, and A2FE) between the two subtypes showed good performance with AUC values greater than 0.8, suggesting that these glycan traits have potential as biomarkers for subtype classification. Observed differences in the serum protein N-glycosylation between indirect IH and direct IH indicate differences in the pathogenesis of these two subtypes. The in-depth mechanisms still need further investigation.

The current study has several limitations. First, as IHs are more common in male than female patients, only male participants were included in this study. Second, the sample sizes of IH (indirect IH and direct IH) patients were relatively small. The potential loss of statistical significance of the glycan traits is likely due to the small sample size and many glycosylation traits being explored, bringing the significance down and warranting larger future studies. If the sample size increases, differentially expressed glycan traits between the subgroups may have better performance in diagnosis or prediction. Third, the results we obtained in this study still need independent validation in large cohorts. Last, further work exploring the molecular mechanisms underlying this result will be needed.

5. Conclusions

To our knowledge, this study reported the total serum N-glycomic features in IH patients for the first time. Furthermore, we identified serum N-glycomic changes specific to IH or IH subtypes, of which eight glycans traits were screened out as candidate biomarkers for diagnosis and subtype classification of IH. Differences in serum protein N-glycosylation reflect differences in pathogenesis between indirect IH and direct IH. These findings can deepen the comprehension of IH.

Funding

Ethics statement

Written informed consent was obtained from the individuals for the publication of potentially identifiable data included in this article. The study was performed according to the guidelines of the Declaration of Helsinki and approved by the Ethics Committee of Peking Union Medical College Hospital and Beijing Chao-Yang Hospital (Ethics Approval Number: K4094; Ethics Approval Date: 2020.05.09).

Informed consent statement

The written informed consent from all participants in the study was provided.

Data availability statement

The original contributions presented in the study are included in the article/Supplementary Material. Further information and requests can be directed to the corresponding author.

CRediT authorship contribution statement

Zhen Cao: Writing – original draft, Validation, Investigation, Conceptualization. **Zejian Zhang:** Validation, Investigation, Data curation. **Yuanyang Wang:** Investigation, Data curation. **Yilin Zhu:** Software, Investigation. **Zepeng Li:** Resources, Investigation. **Xiaobin Li:** Supervision, Resources, Conceptualization. **Yingmo Shen:** Supervision, Resources. **Jie Chen:** Supervision, Resources, Conceptualization. **Ziwen Liu:** Writing – review & editing, Project administration, Funding acquisition, Conceptualization.

Declaration of competing interest

The authors declare that they have no known competing financial interests or personal relationships that could have appeared to influence the work reported in this paper.

Appendix A. Supplementary data

Supplementary data to this article can be found online at https://doi.org/10.1016/j.heliyon.2024.e35908.

References

[1] L. Chung, J. Norrie, P.J. O'Dwyer, Long-term follow-up of patients with a painless inguinal hernia from a randomized clinical trial, Br. J. Surg. 98 (4) (2011) 596–599.
[2] R.D. Matthews, L. Neumayer, Inguinal hernia in the 21st century: an evidence-based review, Curr. Probl. Surg. 45 (4) (2008) 261–312.
[3] R. Bittner, Laparoscopic view of surgical anatomy of the groin, Int J Abdom Wall Hernia Surg 1 (1) (2018) 24–31.
[4] Y. Mao, L. Chen, J. Li, A.J. Shangguan, S. Kujawa, H. Zhao, A network analysis revealed the essential and common downstream proteins related to inguinal hernia, PLoS One 15 (1) (2020) e0226885.
[5] B. Zhao, Z. Wan, J. Wang, H. Liu, Y. Zhou, W. Chen, et al., Comprehensive analysis reveals a six-gene signature and associated drugs in mimic inguinal hernia model, Hernia 24 (6) (2020) 1211–1219.
[6] J.J. Pilkington, T.W. Davies, O. Schaff, M.Y. Alexander, J. Pritchett, F.L. Wilkinson, et al., Systemic biomarkers currently implicated in the formation of abdominal wall hernia: a systematic review of the literature, Am. J. Surg. 222 (1) (2021) 56–66.
[7] G.W. Hart, R.J. Copeland, Glycomics hits the big time, Cell 143 (5) (2010) 672–676.
[8] K. Ohtsubo, J.D. Marth, Glycosylation in cellular mechanisms of health and disease, Cell 126 (5) (2006) 855–867.
[9] K.W. Moremen, M. Tiemeyer, A.V. Nairn, Vertebrate protein glycosylation: diversity, synthesis and function, Nat. Rev. Mol. Cell Biol. 13 (7) (2012) 448–462.
[10] K.K. Palaniappan, C.R. Bertozzi, Chemical glycoproteomics, Chem Rev. 116 (23) (2016) 14277–14306.
[11] A. Varki, Biological roles of glycans, Glycobiology 27 (1) (2017) 3–49.
[12] F. Clerc, M. Novokmet, V. Dotz, K.R. Reiding, N. de Haan, G.S.M. Kammeijer, et al., Plasma N-glycan signatures are associated with features of inflammatory bowel diseases, Gastroenterology 155 (3) (2018) 829–843.
[13] Z. Zhang, M. Westhrin, A. Bondt, M. Wuhrer, T. Standal, S. Holst, Serum protein N-glycosylation changes in multiple myeloma, Biochim. Biophys. Acta Gen. Subj. 1863 (5) (2019) 960–970.
[14] R.K. Kam, T.C. Poon, H.L. Chan, N. Wong, A.Y. Hui, J.J. Sung, High-throughput quantitative profiling of serum N-glycome by MALDI-TOF mass spectrometry and N-glycomic fingerprint of liver fibrosis, Clin. Chem. 53 (7) (2007) 1254–1263.
[15] R. Testa, V. Vanhooren, A.R. Bonfigli, M. Boemi, F. Olivieri, A. Ceriello, et al., N-glycomic changes in serum proteins in type 2 diabetes mellitus correlate with complications and with metabolic syndrome parameters, PLoS One 10 (3) (2015) e0119983.
[16] Y. Wu, Y. Chen, H. Chen, C. Yang, X. Shen, C. Deng, et al., Probing serum N-glycan patterns for rapid and precise detection of Crohn's disease, Chem. Commun. 57 (86) (2021) 11362–11365.
[17] G.C.M. Vreeker, R.G. Hanna-Sawires, Y. Mohammed, M.R. Bladergroen, S. Nicolardi, V. Dotz, et al., Serum N-Glycome analysis reveals pancreatic cancer disease signatures, Cancer Med. 9 (22) (2020) 8519–8529.
[18] K.R. Reiding, D. Blank, D.M. Kuijper, M. Wuhrer, High-throughput profiling of protein N-glycosylation by MALDI-TOF-MS employing linkage-specific sialic acid esterification, Anal. Chem. 86 (12) (2014) 5784–5793.
[19] B.C. Jansen, K.R. Reiding, A. Bondt, A.L. Hipgrave Ederveen, M. Palmblad, D. Falck, et al., MassyTools: a high-throughput targeted data processing tool for relative quantitation and quality control developed for glycomic and glycoproteomic MALDI-MS, J. Proteome Res. 14 (12) (2015) 5088–5098.
[20] A. Ceroni, K. Maass, H. Geyer, R. Geyer, A. Dell, S.M. Haslam, GlycoWorkbench: a tool for the computer-assisted annotation of mass spectra of glycans, J. Proteome Res. 7 (4) (2008) 1650–1659.
[21] Z. Pang, G. Zhou, J. Ewald, L. Chang, O. Hacariz, N. Basu, et al., Using MetaboAnalyst 5.0 for LC-HRMS spectra processing, multi-omics integration and covariate adjustment of global metabolomics data, Nat. Protoc. 17 (8) (2022) 1735–1761.
[22] M.R. Bladergroen, K.R. Reiding, A.L. Hipgrave Ederveen, G.C. Vreeker, F. Clerc, S. Holst, et al., Automation of high-throughput mass spectrometry-based plasma N-glycome analysis with linkage-specific sialic acid esterification, J. Proteome Res. 14 (9) (2015) 4080–4086.
[23] D.S. Graham, I.T. MacQueen, D.C. Chen, Inguinal neuroanatomy: implications for prevention of chronic postinguinal hernia pain, Int J Abdom Wall Hernia Surg 1 (1) (2018) 1–8.
[24] P.J. Tenzel, J.A. Bilezikian, F.E. Eckhauser, W.W. Hope, Tension measurements in abdominal wall hernia repair: concept and clinical applications, Int J Abdom Wall Hernia Surg 2 (4) (2019) 119–124.

[25] A.A. Darwish, A.A. Hegab, Tack fixation versus nonfixation of mesh in laparoscopic transabdominal preperitonaeal hernia repair, Int J Abdom Wall Hernia Surg 35 (4) (2016) 327–331.

[26] G. HerniaSurge, International guidelines for groin hernia management, Hernia 22 (1) (2018) 1–165.

[27] C. Huang, X. Xu, M. Wang, X. Xiao, C. Cheng, J. Ji, et al., Serum N-glycan fingerprint helps to discriminate intrahepatic cholangiocarcinoma from hepatocellular carcinoma, Electrophoresis 42 (11) (2021) 1187–1195.

[28] R. Saldova, V.D. Haakensen, E. Rodland, I. Walsh, H. Stockmann, O. Engebraaten, et al., Serum N-glycome alterations in breast cancer during multimodal treatment and follow-up, Mol. Oncol. 11 (10) (2017) 1361–1379.

[29] S.H. Wang, T.J. Wu, C.W. Lee, J. Yu, Dissecting the conformation of glycans and their interactions with proteins, J. Biomed. Sci. 27 (1) (2020) 93.

[30] H.H. Freeze, R. Steet, T. Suzuki, T. Kinoshita, R.L. Schnaar, Genetic disorders of glycan degradation, in: A. Varki, R.D. Cummings, J.D. Esko, P. Stanley, G. W. Hart, et al. (Eds.), Essentials of Glycobiology, 2022, pp. 583–598. Cold Spring Harbor (NY).

[31] R. Sackstein, K.M. Hoffmeister, S.R. Stowell, T. Kinoshita, A. Varki, H.H. Freeze, Glycans in acquired human diseases, in: A. Varki, R.D. Cummings, J.D. Esko, P. Stanley, G.W. Hart, et al. (Eds.), Essentials of Glycobiology, 2022, pp. 615–630. Cold Spring Harbor (NY).

[32] P. Carpintero-Fernandez, M. Varela-Eirin, A. Lacetera, R. Gago-Fuentes, E. Fonseca, S. Martin-Santamaria, et al., New therapeutic strategies for osteoarthritis by targeting sialic acid receptors, Biomolecules 10 (4) (2020).

[33] M. Cevik, P. Yazgan, N. Aksoy, Evaluation of antioxidative/oxidative status and prolidase parameters in cases of inguinal hernia with joint hypermobility syndrome, Hernia 18 (6) (2014) 849–853.

[34] M. Catera, V. Borelli, N. Malagolini, M. Chiricolo, G. Venturi, C.A. Reis, et al., Identification of novel plasma glycosylation-associated markers of aging, Oncotarget 7 (7) (2016) 7455–7468.

[35] F. Dall'Olio, V. Vanhooren, C.C. Chen, P.E. Slagboom, M. Wuhrer, C. Franceschi, N-glycomic biomarkers of biological aging and longevity: a link with inflammaging, Ageing Res. Rev. 12 (2) (2013) 685–698.

[36] W. Qin, H. Pei, R. Qin, R. Zhao, J. Han, Z. Zhang, et al., Alteration of serum IgG galactosylation as a potential biomarker for diagnosis of neuroblastoma, J. Cancer 9 (5) (2018) 906–913.

[37] G. Amato, L. Marasa, T. Sciacchitano, S.G. Bell, G. Romano, M.C. Gioviale, et al., Histological findings of the internal inguinal ring in patients having indirect inguinal hernia, Hernia 13 (3) (2009) 259–262.

[38] M. Novokmet, E. Lukic, F. Vuckovic, Z. Ethuric, T. Keser, K. Rajsl, et al., Changes in IgG and total plasma protein glycomes in acute systemic inflammation, Sci. Rep. 4 (2014) 4347.

[39] Y. Abe, C.W. Smith, J.P. Katkin, L.M. Thurmon, X. Xu, L.H. Mendoza, et al., Endothelial alpha 2,6-linked sialic acid inhibits VCAM-1-dependent adhesion under flow conditions, J. Immunol. 163 (5) (1999) 2867–2876.

[40] C.W.L. Dougher, A. Buffone Jr., M.J. Nemeth, M. Nasirikenari, E.E. Irons, P.N. Bogner, et al., The blood-borne sialyltransferase ST6Gal-1 is a negative systemic regulator of granulopoiesis, J. Leukoc. Biol. 102 (2) (2017) 507–516.